

Anticancer potential of novel curcumin analogs towards castrate-resistant prostate cancer

SHULI CHEN¹, MHAIRI NIMICK¹, ANDREW G. CRIDGE², BILL C. HAWKINS³ and RHONDA J. ROSENGREN¹

Departments of ¹Pharmacology and Toxicology, ²Biochemistry and ³Chemistry, University of Otago, Dunedin 9016, New Zealand

Received September 11, 2017; Accepted November 14, 2017

DOI: 10.3892/ijo.2017.4207

Abstract. Prostate cancer is initially sensitive to hormone therapy; however, over time the majority of patients progress to a hormone-insensitive form classified as castration-resistant prostate cancer (CRPC). CRPC is highly metastatic and patients have a poor prognosis. Thus, new drugs for the treatment of this disease are required. In this study, we therefore examined the cytotoxic effects and anticancer mechanism(s) of action of second generation curcumin analogs towards CRPC cells. For this purpose, PC3 and DU145 cells were treated with a series of curcumin analogs at 0-10 μ M for 72 h and cytotoxicity was determined by the sulforhodamine B (SRB) assay. Two compounds, 1-isopropyl-3,5-bis(pyridin-3-ylmethylene)-4-piperidone (RL118) and 1-methyl-3,5-[(6-methoxynaphthalen-2-yl)methylene]-4-piperidone (RL121), were found to have the most potent cytotoxic effect with EC₅₀ values of 0.50 and 0.58 μ M in the PC3 cells and EC₅₀ values of 0.76 and 0.69 μ M in the DU145 cells, respectively. Thus, further experiments were performed focusing on these two compounds. Flow cytometry was performed to determine their effects on the cell cycle and apoptosis. Both analogs increased the number of cells in the G2/M phase of the cell cycle and induced apoptosis. Specifically, in the PC3 cells, RL121 increased the number of cells in the G2/M phase by 86% compared to the control, while RL118 increased the number of cells in the G2/M phase by 42% compared to the control after 24 h. Moreover, both RL118 and RL121 induced the apoptosis of both cell lines. In the DU145 cells, a 38-fold increase in the number of apoptotic cells was elicited by RL118 and a 78-fold increase by RL121 compared to the control. Furthermore, the effects of both analogs on the expression of key proteins involved in cell proliferation were also determined by western blot analysis. The results revealed

that both analogs inhibited the expression of nuclear factor (NF)- κ B (p65/RelA), eukaryotic translation initiation factor 4E-binding protein 1 (4E-BP1), p-4E-BP1, mammalian target of rapamycin (mTOR), p-mTOR, AKT and p-AKT. Thus, the findings of this study provide evidence that RL118 and RL121 have potent anticancer activity against CRPC cells, and both analogs warrant further investigation *in vivo*.

Introduction

Prostate cancer is one of the most frequently diagnosed types of cancer and is the second leading cause of cancer-related mortality in males (1,2). The majority of prostate cancers begin in an androgen-dependent state, and thus, hormonal therapy, including surgical castration and medical/chemical castration has become the standard therapy. However, following androgen deprivation therapy, the tumor re-emerges in a more metastatic form that is no longer responsive to this type of therapy and this cancer is then classified as castration-resistant prostate cancer (CRPC) (3). At this stage, the cancer has become incurable and the average survival time of patients is only 16-18 months (4). Moreover, therapeutic strategies have had little effect on the progression of the disease. Therefore, novel treatment strategies and new drug options are urgently required for patients with CRPC.

Curcumin (diferuloylmethane), a polyphenol phytochemical extracted from the plant, *Curcuma longa*, is widely used in Southeast Asia, China and India in food preparation and for medicinal purposes, such as health maintenance and cancer prevention. Due to its anticancer and anti-angiogenic properties, as well as its lack of toxicity and high affordability, curcumin has been extensively studied as a chemotherapeutic agent (5-7). In particular, curcumin has been shown to be cytotoxic towards both the androgen-dependent prostate cancer cell line, LNCaP and the androgen-independent cell lines, DU145 and PC3 (8-10). However, various experimental studies and clinical trials have shown that the systemic bioavailability of orally administered curcumin is low. Serum concentrations often do not reach >0.1% of intake and curcumin exhibits rapid elimination in the feces, bile and urine (11). In order to overcome this limitation, different strategies, including the design and synthesis of structural analogs have been explored. For example, the novel synthetic curcumin analogue, 3,5-bis(2-fluorobenzylidene)-4-piperidone (EF24), has been

Correspondence to: Professor Rhonda J. Rosengren, Department of Pharmacology and Toxicology, University of Otago, 18 Frederick Street, Dunedin 9016, New Zealand
E-mail: rhonda.rosengren@otago.ac.nz

Key words: castrate-resistant prostate cancer, curcumin analogs, PC3 cells, DU145 cells

shown to exhibit improved anticancer properties *in vitro* and *in vivo* compared to curcumin (12). It has been found that 10 μM of EF24 is cytotoxic toward 70-80% of DU145 human prostate cancer cells (12). Pyridine analogs of curcumin with a tetrahydrothiopyrane-4-one linker, analogs FN1, FN2 and FN3, have also exhibited potent anticancer activities in PC3 cells showing a potent inhibitory effect on growth and a potent stimulatory effect on apoptosis at low concentrations ($\leq 1 \mu\text{M}$) (13).

Previously, our group synthesized a series of heterocyclic cyclohexanone analogs of curcumin and investigated their inhibitory activity against nuclear factor (NF)- κB transactivation in non-adherent K562 leukemia cells, as well as cytotoxicity toward ER-negative breast cancer cell lines (14). It has been found that curcumin analogs exhibited potent cytotoxicity towards a variety of breast cancer cell lines. In particular, 1-methyl-3,5-bis(4-pyridyl)methylidene-4-piperidone (RL66) was shown to exhibit EC_{50} values of 0.8, 0.5 and 0.6 μM , while 3,5-bis(3,4,5-trimethoxybenzylidene)-1-methylpiperidine-4-one (RL71) produced EC_{50} values of 0.3, 0.3 and 0.4 μM in MDA-MB-231, MDA-MB-468 and SKBr3 cells, respectively (14). Moreover, both compounds have been shown to significantly increase the number of cells undergoing apoptosis (15,16). Furthermore, both analogs have been shown to decrease HER2/neu phosphorylation and increase p27 levels in SKBr3 cells, while significantly decreasing AKT phosphorylation and transiently increasing the stress kinases c-Jun N-terminal kinase (JNK)1/2 and mitogen-activated protein kinase (MAPK) p38 in MDA-MB-231 and MDA-MB-468 cells (15,16). In the present study, we explored the cytotoxic effects and anticancer mechanisms of a novel series of curcumin analogs towards androgen-independent PC3 and DU145 prostate cancer cells. The initial screening revealed that two curcumin analogs termed 1-isopropyl-3,5-bis(pyridin-3-ylmethylene)-4-piperidone (RL118) and 1-methyl-3,5-[(6-methoxynaphthalen-2-yl)methylene]-4-piperidone (RL121) (Fig. 1) elicited potent cytotoxicity towards the CRPC cell lines. Thus, these two compounds were selected for further experimentation. The results demonstrated that these two curcumin analogs induced cell cycle arrest and apoptosis. Moreover, the results of western blot analysis demonstrated that both analogs modulated the expression of key cell signaling proteins involved in cell proliferation and cell death. Thus, our findings provide evidence that RL118 and RL121 have potent anticancer activity against CRPC cells, and both analogs warrant further examination *in vivo*.

Materials and methods

Materials. The PC3 and DU145 prostate cancer cells and NIH/3T3 mouse embryonic fibroblasts were purchased from the American Type Culture Collection (Manassas, VA, USA). PNT1A normal human prostate epithelial cells were purchased from the European Collection of Authenticated Cell Cultures which is operated by Public Health England (Salisbury, UK). Dulbecco's modified Eagle's medium (DMEM) nutrient mixture Ham's F-12, Eagle's Minimum Essential Medium (EMEM), sulforhodamine B salt, propidium iodide (PI), ammonium persulfate, horseradish peroxidase and β -tubulin

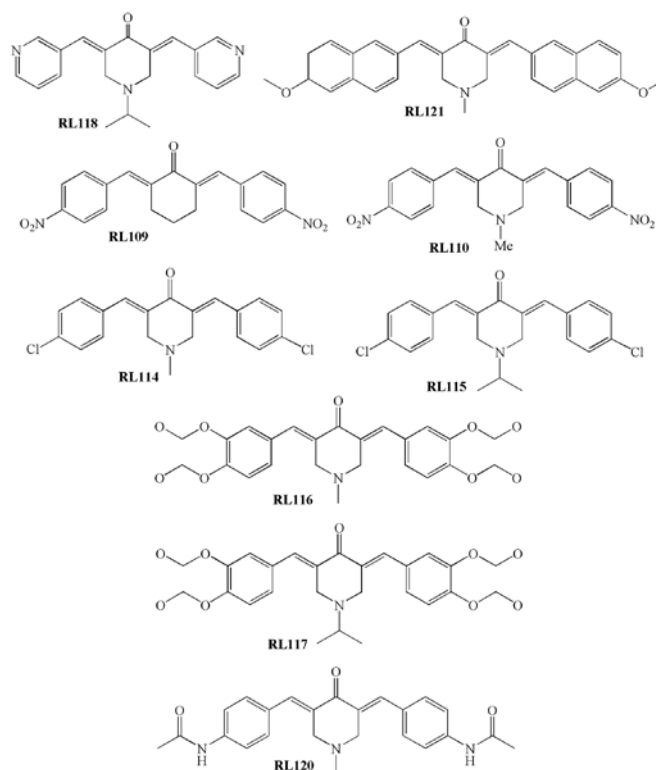


Figure 1. Molecular structures of curcumin analogs.

(cat. no. T5293) were purchased from Sigma-Aldrich (St. Louis, MO, USA). Epidermal growth factor receptor (EGFR; cat. no. 2646), p-EGFR (cat. no. 4404), NF- κB (p65/RelA) (cat. no. 8242), cleaved caspase-3 (cat. no. 9664), eukaryotic translation initiation factor 4E-binding protein 1 (4E-BP1; cat. no. 9452), p-4E-BP1 (cat. no. 9455), mammalian target of rapamycin (mTOR; cat. no. 2972) p-mTOR (cat. no. 2971) primary antibodies were purchased from Cell Signaling Technology (Danvers, MA, USA). AKT (cat. no. 559028) and p-AKT (cat. no. 4058) primary antibodies were purchased from BD Biosciences (Auckland, New Zealand). Goat anti-rabbit horseradish peroxidase (cat. no. 401353) and goat anti-mouse horseradish peroxidase (cat. no. 401253) secondary antibodies were purchased from Merck (Billerica, MA, USA). Acrylamide, bisacrylamide, sodium dodecylsulfate and PVDF membrane were purchased from Bio-Rad Laboratories (Hercules, CA, USA). Complete Mini EDTA-free protease inhibitor cocktail and Annexin-V-FLUOS were purchased from Roche Diagnostics Corp. (Mannheim, Germany). RNase A, bovine serum albumin (BSA) and trypsin were purchased from Invitrogen (Auckland, New Zealand). All synthetic curcumin analogs were synthesized by Dr Bill Hawkins from the Department of Chemistry at the University of Otago, Dunedin, New Zealand.

Synthesis of curcumin derivatives. 1-isopropyl-3,5-bis[(pyridine-3-yl)methylene]piperidin-4-one (RL118) was synthesized as follows: To a solution of 1-isopropylpiperidin-4-one (1.4 g, 10 mmol) and pyridine-3-carboxaldehyde (2.14 g, 20 mmol) in methanol (10 ml) was added a solution of sodium methoxide in methanol (5 M, 1.5 ml) and the mixture was stirred for 18 h. The resultant yellow crystalline solid was

removed by filtration then recrystallized from methanol to yield pure 1-isopropyl-3,5-bis[(pyridine-3-yl)methylene]piperidin-4-one as a yellow crystalline solid (1.45 g, 45%). HRMS (+ve ESI) calculated for $C_{20}H_{21}N_3ONa^+$: 342.1577 m/z. $[MNa^+]$ found 342.1567 m/z. 1-methyl-3,5-bis[(6-methoxy-2-naphthyl)methylene]piperidin-4-one (RL121) was synthesized as follows: To a solution of the *N*-methyl-4-piperidone (0.50 ml, 0.46 g, 4.05 mmol) and 6-methoxy-2-naphthaldehyde (1.51 g, 8.10 mmol) in methanol (10 ml) was added a solution of sodium methoxide in methanol (5 M, 1.0 ml) and the mixture was stirred for 16 h. The resultant solid was collected via filtration to afford the title compound (1.35 g, 74%) as a light brown crystalline solid. 1H NMR (400 MHz, $CDCl_3$), δ (ppm): 8.05, bs, 2H; 7.81-7.76, m, 6H; 7.48, dd, 2H, $J=8.2, 1.5$ Hz; 7.20, dd, 2H, $J=8.4, 2.5$ Hz; 7.15, d, 2H, $J=2.5$ Hz; 4.02, bs, 2H; 3.07, m, 2H; 3.95, s, 6H; 2.55, s, 3H. HRMS-ESI calculated for $C_{30}H_{28}NO_3 + [M+H]^+$: 449.1991; found: 449.1996.

Cell maintenance. The PC3 prostate cancer cells were cultured in DMEM/Ham's F-12 supplemented with 10% FBS, 1% L-glutamine, 1% penicillin/streptomycin and the DU145 cells were maintained in MEM supplemented with 10% fetal bovine serum (FBS), 1% L-glutamine, 1% penicillin/streptomycin. The cells were kept in a humidified incubator at 37°C with 5% CO_2 .

Cytotoxicity. The prostate cancer cells, PC3 and DU145, and the normal human prostate epithelial cells, PNT1A, were seeded in 96-well plates at a rate of 4,000 and 6,000 cells per well, respectively and allowed to adhere to the plate for 24 h at 37°C. The cells were then treated with curcumin analogs with a range of concentrations (0.1-10 μM) of each compound for 72 h. The vehicle control cells were treated with dimethyl sulfoxide (DMSO) (0.1%). The cell number in each well was determined by the sulforhodamine B (SRB) assay (14). Cytotoxicity time course studies were conducted by treating the PC3 and DU145 cells with compounds RL118 or RL121 at 0.5, 0.75, 1, 1.5 or 2 μM for 12-72 h. Data are expressed as the number of viable cells determined from 3 independent experiments conducted in triplicate.

Cell cycle analysis. The PC3 (1.0×10^5 cells per well) and DU145 (2.0×10^5 cells per well) cells were seeded in 6-well plates in 2 ml of complete medium and allowed to adhere to the plate for 24 h. The cells were then treated with RL118 (1 μM for PC3 cells and 2 μM for DU145 cells) or RL121 (1 μM for both cell lines) using 0.1% DMSO as a control for 24 and 48 h. The cells were then harvested, washed with phosphate-buffered saline (PBS) and fixed in 70% ethanol. Following rehydration with PBS, the cells were stained with PI in the dark at 4°C as previously described (17). The samples were analyzed via flow cytometry using a BD FACSCalibur flow cytometer (BD Biosciences, Auckland, New Zealand). Data were acquired and analyzed using FlowJo software. Data are expressed as the mean proportion of cells in each phase \pm SEM determined from 3 independent experiments conducted in triplicate.

Induction of apoptosis. The percentage of PC3 and DU145 cells undergoing apoptosis following treatment with RL118

and RL121 was determined by flow cytometry. The PC3 cells (1.0×10^5 cells per well) and DU145 cells (2.0×10^5 cells per well) were seeded in 6-well plates with 2 ml of complete medium and allowed to adhere to the plate for 24 h. The cells were then treated with RL118 (1 μM for the PC3 cells and 2 μM for the DU145 cells) or RL121 (1 μM for both cell lines) for 24 and 48 h. The vehicle control cells were treated with 0.1% DMSO. Apoptosis was assessed using Annexin-V-FLUOS/PI (Roche Diagnostics Corp.) staining, as previously described (18). The samples were analyzed via flow cytometry using a BD FACSCalibur flow cytometer. Data were acquired and analyzed using FlowJo software. Values are expressed as the number of apoptotic cells as a % of the total number of cells \pm SEM determined from 3 independent experiments conducted in triplicate.

Western blot analysis. The PC3 cells (1.0×10^6 cells per dish) and DU145 cells (2.0×10^6 cells per dish) were seeded in 10-cm cell culture dishes in 10 ml of complete medium and allowed to adhere to the plate for 24 h. The cells were then treated with RL118 (1 μM for the PC3 cells and 2 μM for the DU145 cells), RL121 (1 μM for both cell lines) and the vehicle control (0.1% DMSO) for 24 and 48 h. At the end of treatment, whole cell lysates were prepared and the protein concentration of the lysates was determined using the bicinchoninic acid (BCA) assay as previously described (17). Cell lysates were resolved on a SDS-PAGE gel (1 μg of protein per lane) and transferred onto a PVDF membrane. Protein levels were analyzed with the desired primary antibodies, followed by horseradish peroxidase-conjugated secondary antibodies (Merck). Digital chemiluminescence images were acquired using a VersaDoc (Bio-Rad Laboratories) imaging system and All-PRO Imaging system and quantified using Quantity One software (Bio-Rad Laboratories).

Statistical analysis. When time was a factor, data were analyzed with a two-way ANOVA coupled with a Bonferroni post-hoc test, where $p < 0.05$ was required for a statistically significant difference. When time was not a factor, data were analyzed with a one-way ANOVA coupled with Bonferroni post-hoc test, where $p < 0.05$ was required for a statistically significant difference.

Results

In total, 9 different curcumin analogs namely, RL109, RL110, RL114, RL115, RL116, RL117, RL118, RL120 and RL121 were screened for their cytotoxicity towards the PC3 cells. A total of 5 curcumin analogs elicited EC_{50} values within the range of 0.5-100 μM , while RL120 was unable to elicit an EC_{50} value over the range of concentrations tested (Table I). Since RL118 and RL121 were the most potent compounds towards the PC3 cells (Fig. 2A and B), they were also examined in the DU145 cells, where they exhibited equivalent cytotoxicity (Fig. 2C and D). To determine the selectivity of RL118 and RL121 towards cancer cells, the effects of these compounds on PNT1A non-cancerous prostate cells and NIH/3T3 mouse embryonic fibroblasts were examined. The results revealed that RL118 had EC_{50} values of 9 μM in the NIH/3T3 cells and 1.8 μM in the PNT1A cells (Fig. 3). For RL121, the EC_{50}

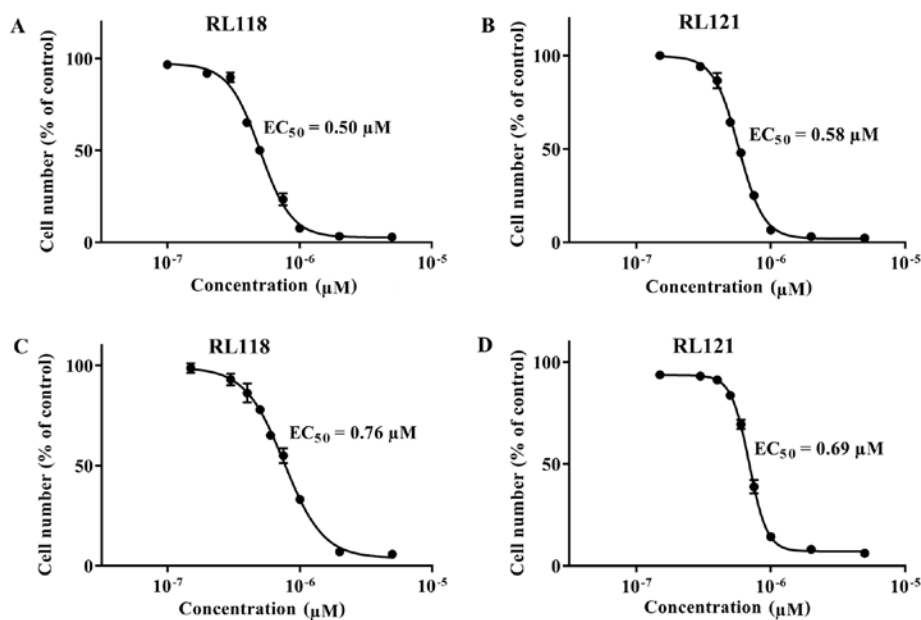


Figure 2. EC_{50} values of RL118 and RL121 in castration-resistant prostate cancer (CRPC) cells. The (A and B) PC3 and (C and D) DU145 cells were treated with 0.1 to 5 μ M of RL118 (A and C) and RL121 (B and D) for 72 h. The vehicle control cells were treated with 0.1% DMSO. At the end of each treatment, the cell number was determined by SRB assay. Symbols represent cell number (% of control) \pm SEM from 3 independent experiments conducted in triplicate. EC_{50} values were obtained using non-linear regression.

Table I. EC_{50} values of curcumin analogs in PC3 cells.

Curcumin analogs	EC_{50} (μ M) ^a
RL109	>100
RL110	2.66 \pm 0.48
RL114	3.09 \pm 0.30
RL115	6.70 \pm 8.52
RL116	12.88 \pm 10
RL118	0.50 \pm 0.05
RL117	1.09 \pm 0.13
RL120	ND ^b
RL121	0.53 \pm 0.03

^aData are represented as the $EC_{50} \pm$ SEM; ^bND, unable to elicit an EC_{50} value within the range of concentrations tested.

values were 3 μ M in the NIH/3T3 cells and 1.5 μ M in the PNT1A cells (Fig. 3). Thus, the two compounds were 3- to 18-fold less potent towards non-cancerous cells compared to the PC3 cells. In order to further investigate the cytotoxicity of the two curcumin analogs, the PC3 and DU145 cells were treated with various concentrations of RL118 and RL121 over a time-course. Time- and concentration-dependent effects were observed for both cell lines. Treatment of the PC3 and DU145 cells with both analogs delayed the growth of cells beginning from 12 h, and this differed significantly compared to the control after 48 h (Fig. 4). The DU145 cells were more resistant to the effects of RL118 as higher concentrations were required to delay cell growth and no concentration was cytotoxic (Fig. 4C).

Cell cycle analysis by flow cytometry was then performed in order to examine whether the cytotoxicity of RL118 and

RL121 was driven by cell cycle arrest. The results revealed that both RL118 and RL121 resulted in a cell line-, time- and dose-dependent cell cycle arrest. Both analogs significantly induced cell cycle arrest in the G2/M phase in the PC3 and DU145 cell lines. Specifically, both RL118 and RL121 led to G2/M phase arrest at 24 and 48 h in the PC3 cells at 1 μ M. Specifically, RL121 induced a significant 86% increase at 24 h and a 57% increase at 48 h, while RL118 caused a significant increase by 42% at 24 h and a 30% increase at 48 h in the number of PC3 cells in G2/M phase arrest compared to the controls (Fig. 5A). Treatment of the DU145 cells with 2 μ M of RL118 and 1 μ M of RL121 exhibited a differential cell cycle effect at both time-points (Fig. 5B). RL118 induced a significant increase in the number of cells in the G2/M phase by 18% at 24 h and 14% at 48 h, compared to the controls. RL121 caused a significant increase in the number of cells in the G2/M phase by 24 and 21% at 24 and 48 h, respectively, compared to the controls.

The ability of RL118 and RL121 to elicit the apoptotic cell death of CRPC cells was then examined. The results revealed that both RL118 and RL121 induced the apoptosis of the PC3 and DU145 cells in a time- and cell line-dependent manner. Specifically, RL118 and RL121 significantly increased the number of apoptotic cells in both cell lines compared to the controls after 48 h (Fig. 6). Moreover, this effect was more potent in the DU145 cells, as >30% of the total number of cells was apoptotic following treatment with RL121 (1 μ M) (Fig. 6B), compared to 20% of the PC3 cells. Apoptosis was also analyzed by quantifying the changes in the levels of cleaved caspase-3 by western blot analysis. Significantly elevated protein levels of cleaved caspase-3 were only elicited by RL121 (1 μ M) and this effect was strongest in the DU145 cells after 24 h of treatment (Fig. 6C and D). Since the activation of NF- κ B leads to cell survival and proliferation, we

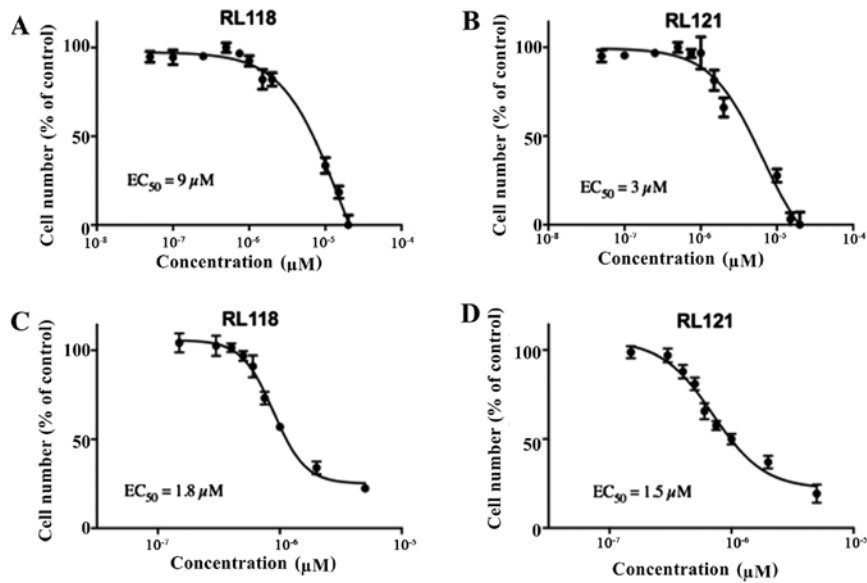


Figure 3. EC_{50} values of RL118 and RL121 in non-cancerous cell lines. (A and B) NIH/3T3 mouse embryonic fibroblasts and (C and D) PTN1A normal human prostate epithelial cells treated were with 0.15 to 20 μ M of RL118 (A and C) and RL121 (B and D) for 72 h. 0.1% DMSO served as the vehicle control. At the end of each treatment, the cell number was determined by SRB assay. Symbols represent cell number (% of control) \pm SEM from 3 independent experiments conducted in triplicate. EC_{50} values were obtained using non-linear regression.

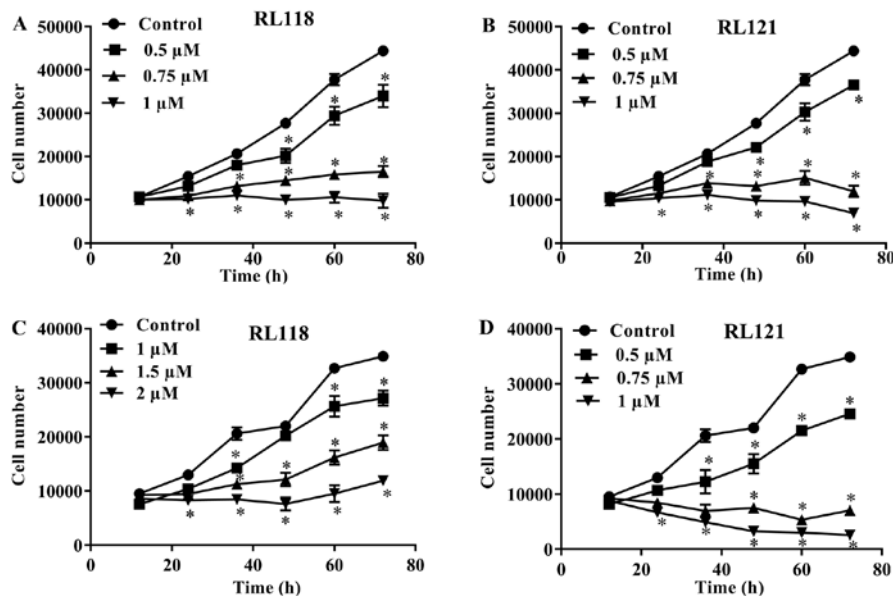


Figure 4. Time course cytotoxicity of RL118 and RL121 in CRPC cells. (A and B) PC3 and (C and D) DU145 cells were treated with RL118 (A and C) and RL121 (B and D) for 12-72 h. The vehicle control cells were treated with 0.1% DMSO. At the end of each treatment, the cell number was determined by SRB assay. Symbols represent cell number (% of control) \pm SEM from 3 independent experiments conducted in triplicate. Data were analyzed using a two-way ANOVA coupled with a Bonferroni post-hoc test. * $p < 0.005$, significantly different from the control.

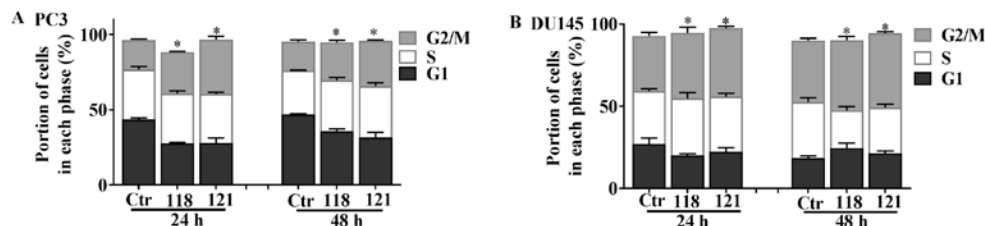


Figure 5. Cell cycle distribution of CRPC cells following treatment with RL118 and RL121. (A) PC3 cells were treated with RL118 (1 μ M) and RL121 (1 μ M), while (B) DU145 cells were treated with RL118 (2 μ M) and RL121 (1 μ M) for 24 and 48 h. Vehicle control cells were treated with 0.1% DMSO. Bars represent the mean proportion of cells in various phases of cell cycle (% of total) \pm SEM of 3 independent experiments conducted in triplicate. Data were analyzed using a two-way ANOVA coupled with a Bonferroni post-hoc test. * $p < 0.05$, significantly different from the control.

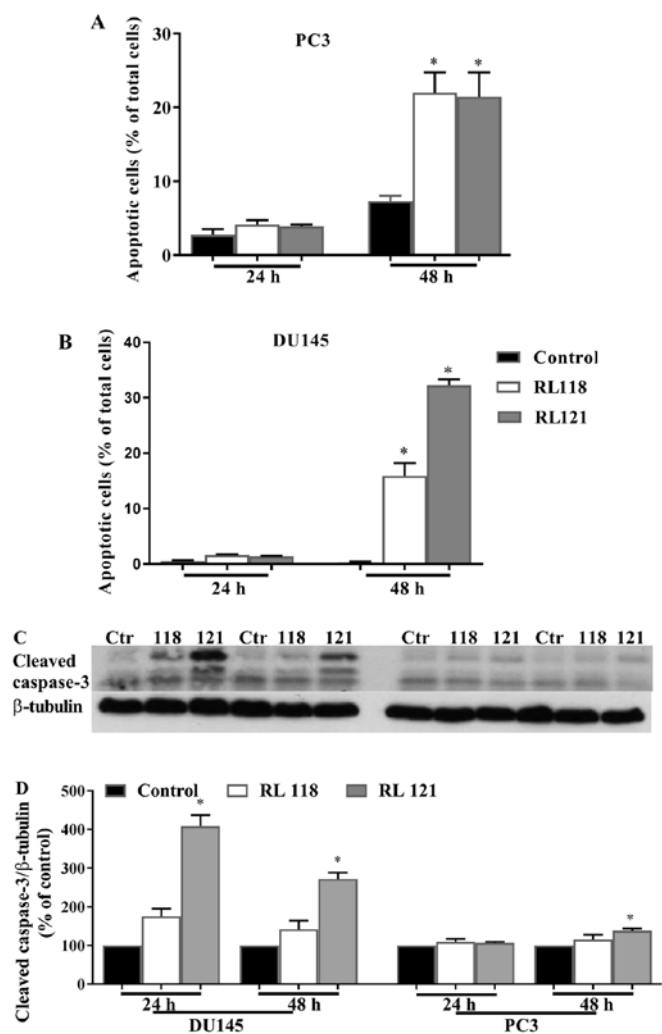


Figure 6. Induction of apoptosis of CRPC cells. (A) PC3 cells were treated with RL118 (1 μ M) and RL121 (1 μ M), while (B) DU145 cells were treated with RL118 (2 μ M) and RL121 (1 μ M) for 24 and 48 h. Vehicle control cells were treated with 0.1% DMSO. Representative western blot analysis for cleaved caspase-3 and β -tubulin served as the loading control (C). Scanning densitometry of western blots for cleaved caspase-3 (D). Bars represent the mean \pm SEM from 3 independent experiments conducted in triplicate. Data were analyzed using a two-way ANOVA coupled with a Bonferroni post-hoc test. * p <0.001, significantly different from the control.

examined the effects of the two compounds on the expression of this protein. RL121 (1 μ M) significantly decreased NF- κ B (p65/RelA) expression by 28 and 42% in the DU145 and PC3 cells, respectively after 24 h and this effect continued for 48 h (Fig. 7A and B). A similar effect was observed with RL118 except that after 48 h, no significant change in the expression of NF- κ B (p65/RelA) was observed in either cell line.

To account for these differences between RL118 and RL121, we examined changes in the protein expression of EGFR. The results revealed that the PC3 cells were the most susceptible to the effects of RL121, as EGFR expression was decreased by 71 and 62% after 24 and 48 h, respectively, while the ratio of p-EGFR/EGFR was significantly increased (Fig. 7). Of note, in the DU145 cells, this relative increase in p-EGFR did not occur and this is likely due to the fact that DU145 cells express phosphatase and tensin homolog (PTEN), whereas PC3 cells lack this protein (19). Further analysis of

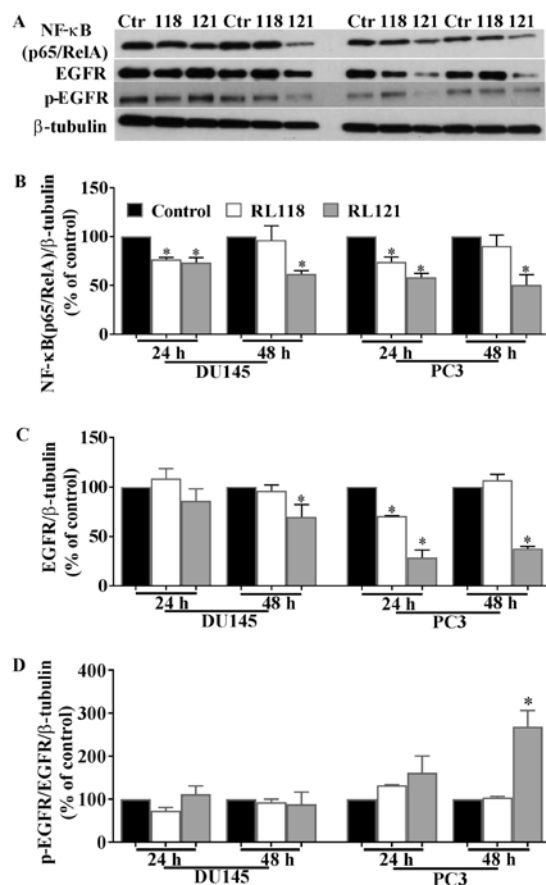


Figure 7. Effect of RL118 and RL121 on NF- κ B (p65/RelA) and EGFR in CRPC cells. PC3 and DU145 cells were treated with RL118 (1 or 2 μ M), RL121 (1 μ M) or vehicle control (0.1% DMSO) for 24 and 48 h. Cell lysates were examined by western blot analysis and β -tubulin was used as the loading control. (A) Representative blots for each protein, cell line and time-point, and scanning densitometry of (B) NF- κ B (p65/RelA), (C) EGFR and (D) p-EGFR/EGFR. Bars represent the means \pm SEM from 3 independent experiments performed in triplicate. Data were analyzed using a one-way ANOVA coupled with a Bonferroni post-hoc test. * p <0.05, significantly different from the control.

the impact that changes in PTEN expression may have on these cells were then conducted by examining changes in the levels of AKT, mTOR and 4E-BP1. Since no changes in EGFR expression were observed after 24 h in the DU145 cells, further investigations focused on treatment after 48 h in this cell line, while experiments with PC3 cells utilized both the 24 and 48 h time-points.

An important cell signaling hub downstream of the EGFR is AKT and thus this was examined as the next mechanistic protein. The results revealed that the PC3 cells were the most susceptible to the effects of RL121, as this compound directly inhibited AKT beginning at 24 h (Fig. 8A and B). Specifically, the ratio of p-AKT/AKT significantly decreased by 39 and 73% compared to the controls at 24 and 28 h, respectively (Fig. 8A and B). The DU145 cells were unresponsive to treatment and RL118 was unable to significantly inhibit AKT regardless of the cell line examined. AKT activation leads to the phosphorylation of mTOR, which subsequently phosphorylates 4E-BP1. Therefore, western blot analysis was carried out to examine the effects of RL118 and RL121 on the expression of mTOR, p-mTOR, 4E-BP1 and phosphorylated

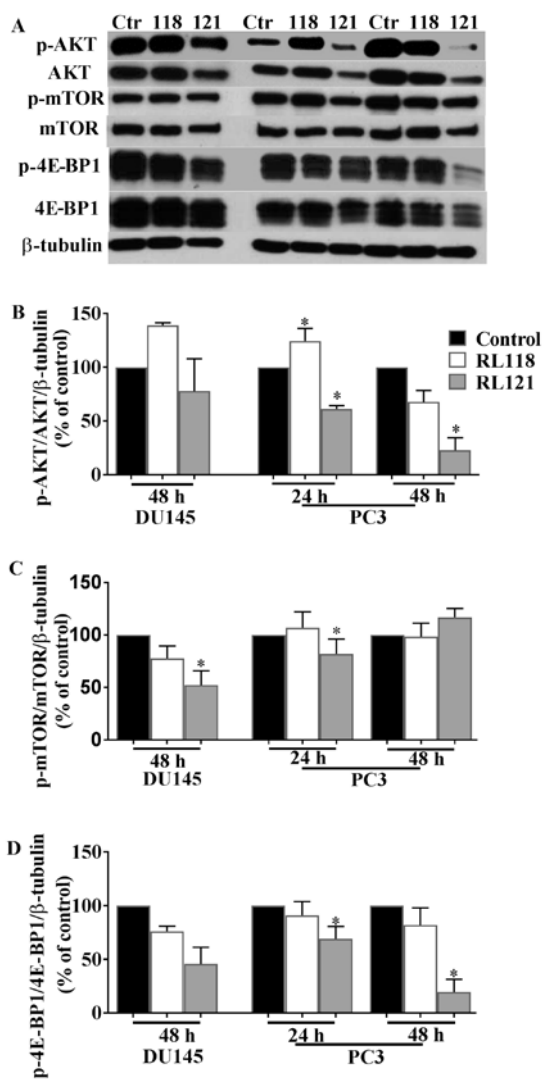


Figure 8. RL118 and RL121 modulates the expression of proteins essential for CRPC cancer cell proliferation and translation. PC3 and DU145 cells were then treated with RL118 (1 or 2 μ M), RL121 (1 μ M) or vehicle control (0.1% DMSO) and incubated for 24 and 48 h. Cell lysates were examined by western blot analysis and β -tubulin was used as the loading control. (A) Representative blots for each protein, cell line and time-point, and scanning densitometry of (B) p-Akt/Akt, (C) p-mTOR/mTOR and (D) p-4E-BP1/4E-BP1. Bars represent the means \pm SEM from 3 independent experiments performed in triplicate. Data were analyzed using a one-way ANOVA coupled with a Bonferroni post-hoc test. * p <0.05, significantly different from the control.

4E-BP1 in the PC3 and DU145 cell lines. Of note, mTOR protein expression was unaltered in the PC3 cells in contrast to their prior high susceptibility to AKT. The only significant decrease in the ratio of p-mTOR/mTOR was observed in the DU145 cells following treatment with RL121 for 48 h, where a decrease of 48% compared to the controls was observed (Fig. 8A and C). This change correlated with a 55% decrease in the ratio of p4E-BP1/4E-BP1 in the DU145 cells compared to the controls following 48 h of treatment with RL121 (Fig. 7A and D). The PC3 cells exhibited the most significant decrease in the ratio of p4E-BP1/4E-BP1, where RL121 significantly decreased the expression of p-4E-BP1/4E-BP1 by 81% compared to the controls after 48 h. Overall, of the two curcumin derivatives, RL121 produced a stronger and

more consistent effect on cell signaling-related proteins in the PC3 cells.

Discussion

In this study, in order to identify potent novel potential drugs for the treatment of CRPC, 9 different curcumin analogs were evaluated for their cytotoxicity towards the PC3 cells. While RL118 and RL121 exhibited the most potent cytotoxicity towards the PC3 cells, these two analogs exhibited a slightly lower potency in the DU145 cells. This may be due in part to the fact that PC3 cells have a higher metastatic potential than DU145 cells. Additionally, time-course experiments revealed that RL121 was cytotoxic, while RL118 was cytostatic. It has been reported that curcumin analogs containing a cyclohexanone or *N*-methylpiperidone core exhibit enhanced potency compared to other curcumin analogs in PC3 and DU145 cells (20). Indeed, we have previously found that 2,6-bis(pyridin-4-ylmethylene)-cyclohexanone (RL91), which contains a cyclohexanone core, exhibited high potency in PC3 and DU145 cells with EC_{50} values of 2.4 and 2.1 μ M, respectively (21). However, RL118 and RL121 were more potent than RL91 in both cell lines. This may be due to the fact that both RL118 and RL121 incorporate an *N*-methylpiperidone core. In our previous study, on the structure-activity relationship of curcumin analogs, the *N*-methylpiperidone analogs 3,5-bis(pyridine-4-yl)-1-methylpiperidin-4-one (RL66) and 3,5-bis(3,4,5-trimethoxybenzylidene)-1-methylpiperidin-4-one (RL71) exhibited potent cytotoxicity with EC_{50} values of 0.3 and 0.8 μ M in the MDA-MB-231 cells, respectively (14). While in the same cell line, the EC_{50} values of cyclohexanone containing analogs were >1 μ M (14). RL118 and RL121 also elicited more potent cytotoxicity in CRPC cells compared to the amono-carbonyl containing derivative, WZ35 (22) and the mono-ketone derivatives FLLL11 and FLLL12 (23).

RL121 was a more potent inducer of G2/M-phase arrest in both cell lines than RL118. G2/M phase cell cycle arrest is a common response following curcumin and many of its analogs (15,16,21-24) and this arrest often is not the driver of apoptosis. It does however, lead to a sustained and potent apoptotic effect (12,13). This was also shown by RL121, as >25% of the cell population of both PC3 and DU145 cells was apoptotic by 48 h. Apoptosis, in contrast to necrosis, is characterized as active and programmed cell death with distinct morphological changes via energy-dependent biochemical mechanisms (25). The loss or suppression of apoptosis correlates with the progression of prostate cancer; therefore, the induction of apoptosis has been considered an effective therapeutic approach for the treatment of prostate tumors (26). Not surprisingly, RL118 and RL121 were both more effective at inducing apoptosis than other curcumin derivatives, such as WZ35 (22), compound 17 (27), EF24 (12), A2 and A4 (28), as all required concentrations between 2.5-20 μ M in order to significantly increase the number of apoptotic CRPC cells or significantly increase the activity of caspase-3.

As an important class of transcriptional regulators, NF- κ B plays a pivotal role in the regulation of cell growth, apoptosis, angiogenesis and metastasis (29-31). The overexpression of NF- κ B has been observed in prostate cancer cell lines and clinically (32-34). Activation of NF- κ B in the nucleus of pros-

tate cancer cells was associated with chemoresistance, PSA recurrence and metastatic spread of prostate cancer (35-37). Furthermore, the inhibition of NF- κ B activity is required to induce the apoptosis of both PC3 and DU145 cells (38). Moreover, a recent study showed that the activation of NF- κ B signaling in prostate cancer cells increased the expression of osteoclastogenic genes which subsequently resulted in bone metastases formation (39). Therefore, targeting NF- κ B may prove to be a potent therapeutic target for CRPC. A previous study revealed that transfected PC3 cells in which NF- κ B activity was blocked, produced slow-growing tumors with a low metastatic potential (40). RL121 was more consistent at inhibiting NF- κ B (p65/RelA) protein expression in CRPC cells and again was more potent than other analogs, such as EF24 (41) and EF31 (42), both of which contain the same piperidone core as RL118 and RL121.

EGFR plays a key role in the proliferation, migration and invasion of tumor cells in prostate tumor progression (43). In particular, EGFR is frequently overexpressed in prostate cancer and is associated with a poor prognosis (44). For example, the frequency of EGFR expression increased from 41% in patients with localized disease to 100% in patients with castrate-resistant metastatic prostate cancer (45). Previously, combination experiments with curcumin (25 μ M) and β -phenylethyl isothiocyanate (PEITC) (10 μ M) significantly suppressed p-EGFR (Y1068) protein by 86% of the control in PC3 cells (46). In this study, treatment with RL121 for 48 h significantly inhibited EGFR expression, but increased the ratio of p-EGFR/EGFR in the PC3 cells, but not the DU145 cells. This may be due to the fact that PC3 cells are PTEN-negative. PTEN controls endocytic trafficking of EGFR by promoting late endosome maturation and is required for the transition of ligand-bound EGFR from early to late endosomes. The depletion of PTEN delays EGFR trafficking and degradation (47). The slower kinetics of receptor degradation will likely affect the rates of EGFR and p-EGFR differentially as p-EGFR cycling is activated upon ligand binding which directs the internalization of these receptors to early endosome to the multivesicular body and then on to the lysosome. When PTEN is present, the accumulation of EGFRs on the limiting membrane of the endosomes is sufficient to produce EGFR-dependent apoptosis (48). The deletion of PTEN delays this process and may uncouple it from apoptosis-induced EGFR degradation. Hence, this is likely the reason for the relative increase in p-EGFR following RL121 treatment in PC3 cells at 48 h compared to DU145-treated cells.

The serine-threonine kinase AKT is an important regulator of protein synthesis and cell cycle progression (49,50). Accumulating evidence has indicated that overexpressed AKT and p-AKT activity has been associated with prostate cancer progression (51-56). The combination of curcumin (25 μ M) and PEITC (10 μ M) has been shown to inhibit the expression of AKT and levels of p-AKT in PC3 cells (46). Moreover, the curcumin analogue, FLLL12, has been shown to inhibit p-AKT expression in PC3 cells (23). RL121 is a more potent and direct inhibitor of AKT, as 1 μ M significantly decreased the ratio of p-AKT/AKT in PC3 cells. This is a critical action of RL112 as, when PTEN is absent, there is an increase in the signaling through both the RAS/RAF/MEK/ERK and

AKT/mTOR pathways (57) and thus these pathways would dominate. Therefore, the direct inhibition of AKT will be an important driver of cell death in PC3 cells and will also drive the decrease observed in NF- κ B (p65/RelA) following RL112 treatment.

mTOR, a member of the PI3K kinase superfamily, plays a key role in the regulation of protein synthesis, cell growth, proliferation, differentiation and survival (58). In a previous study, immunohistochemical analysis revealed that the expression of mTOR and cytoplasmic p-mTOR was significantly increased in prostate cancer tissue compared to the normal prostatic epithelium with mTOR levels in cancer cells being 2-fold higher than those in benign tissue (59). In this study, RL118 had no effect on mTOR levels; however, by contrast, RL121 decreased the ratio of p4E-BP1/4E-BP1 protein levels by 55% in DU145 cells and 81% in PC3 cells. It is not likely that RL121 inhibited 4E-BP1 directly as in the DU145 cells, the 55% decrease in the ratio of p4E-BP1/4E-BP1 levels correlated with a 48% decrease in the ratio of p-mTOR/mTOR, most likely directed through the inhibition of AKT. As stated previously in PC3 cells, when PTEN is absent, there is an increase in signaling through the RAS/RAF/MEK/ERK pathways as well as the AKT/mTOR pathway (57). It is likely that ERK can act directly on 4E-BP1 and indirectly via TSC2/mTOR, as following ionizing radiation, it has been shown to stimulate protein synthesis via ATM-dependent ERK phosphorylation (60,61). Thus, in PC3 cells, the ratio of p-4E-BP1/4E-BP1 changes independently of changes in mTOR. Therefore, RL121 has several advantages in PC3 cells as it can modulate changes in AKT directly and also decrease the in ratio of p4E-BP1/4-EBP1 in an environment of highly active mTOR. Of the 9 novel curcumin analogs screened, RL118 and RL121 exhibited the most potent anticancer activity in the PC3 and DU145 cell lines. While both analogs warrant further examination *in vivo*, RL121 has a wider range of activity in prostate cancers that lack PTEN, and may thus be considered to be the lead compound to emerge from this study.

References

1. Greenlee RT, Murray T, Bolden S and Wingo PA: Cancer statistics, 2000. *CA Cancer J Clin* 50: 7-33, 2000.
2. Siegel R, Ward E, Brawley O and Jemal A: Cancer statistics, 2011: The impact of eliminating socioeconomic and racial disparities on premature cancer deaths. *CA Cancer J Clin* 61: 212-236, 2011.
3. Karantanos T, Corn PG and Thompson TC: Prostate cancer progression after androgen deprivation therapy: Mechanisms of castrate resistance and novel therapeutic approaches. *Oncogene* 32: 5501-5511, 2013.
4. Marques RB, Dits NF, Erkens-Schulze S, van Weerden WM and Jenster G: Bypass mechanisms of the androgen receptor pathway in therapy-resistant prostate cancer cell models. *PLoS One* 5: e13500, 2010.
5. Shakibaei M, Mobasheri A, Lueders C, Busch F, Shayan P and Goel A: Curcumin enhances the effect of chemotherapy against colorectal cancer cells by inhibition of NF- κ B and Src protein kinase signaling pathways. *PLoS One* 8: e57218, 2013.
6. Sadzuka Y, Nagamine M, Toyooka T, Ibuki Y and Sonobe T: Beneficial effects of curcumin on antitumor activity and adverse reactions of doxorubicin. *Int J Pharm* 432: 42-49, 2012.
7. Chuang SE, Kuo ML, Hsu CH, Chen CR, Lin JK, Lai GM, Hsieh CY and Cheng AL: Curcumin-containing diet inhibits diethylnitrosamine-induced murine hepatocarcinogenesis. *Carcinogenesis* 21: 331-335, 2000.

8. Strimpakos AS and Sharma RA: Curcumin: Preventive and therapeutic properties in laboratory studies and clinical trials. *Antioxid Redox Signal* 10: 511-545, 2008.
9. Khor TO, Keum YS, Lin W, Kim JH, Hu R, Shen G, Xu C, Gopalakrishnan A, Reddy B, Zheng X, *et al*: Combined inhibitory effects of curcumin and phenethyl isothiocyanate on the growth of human PC-3 prostate xenografts in immunodeficient mice. *Cancer Res* 66: 613-621, 2006.
10. Dorai T, Gehani N and Katz A: Therapeutic potential of curcumin in human prostate cancer-I. curcumin induces apoptosis in both androgen-dependent and androgen-independent prostate cancer cells. *Prostate Cancer Prostatic Dis* 3: 84-93, 2000.
11. Anand P, Kunnumakkara AB, Newman RA and Aggarwal BB: Bioavailability of curcumin: Problems and promises. *Mol Pharm* 4: 807-818, 2007.
12. Adams BK, Cai J, Armstrong J, Herold M, Lu YJ, Sun A, Snyder JP, Liotta DC, Jones DP and Shoji M: EF24, a novel synthetic curcumin analog, induces apoptosis in cancer cells via a redox-dependent mechanism. *Anticancer Drugs* 16: 263-275, 2005.
13. Wei X, Zhou D, Wang H, Ding N, Cui XX, Wang H, Verano M, Zhang K, Conney AH, Zheng X, *et al*: Effects of pyridine analogs of curcumin on growth, apoptosis and NF- κ B activity in prostate cancer PC-3 cells. *Anticancer Res* 33: 1343-1350, 2013.
14. Yadav B, Taurin S, Rosengren RJ, Schumacher M, Diederich M, Somers-Edgar TJ and Larsen L: Synthesis and cytotoxic potential of heterocyclic cyclohexanone analogues of curcumin. *Bioorg Med Chem* 18: 6701-6707, 2010.
15. Yadav B, Taurin S, Larsen L and Rosengren RJ: RL66 a second-generation curcumin analog has potent *in vivo* and *in vitro* anticancer activity in ER-negative breast cancer models. *Int J Oncol* 41: 1723-1732, 2012.
16. Yadav B, Taurin S, Larsen L and Rosengren RJ: RL71, a second-generation curcumin analog, induces apoptosis and downregulates Akt in ER-negative breast cancer cells. *Int J Oncol* 41: 1119-1127, 2012.
17. Somers-Edgar TJ, Taurin S, Larsen L, Chandramouli A, Nelson MA and Rosengren RJ: Mechanisms for the activity of heterocyclic cyclohexanone curcumin derivatives in estrogen receptor negative human breast cancer cell lines. *Invest New Drugs* 29: 87-97, 2011.
18. Stuart EC, Jarvis RM and Rosengren RJ: In vitro mechanism of action for the cytotoxicity elicited by the combination of epigallocatechin gallate and raloxifene in MDA-MB-231 cells. *Oncol Rep* 24: 779-785, 2010.
19. Beresford SA, Davies MA, Gallick GE and Donato NJ: Differential effects of phosphatidylinositol-3/Akt-kinase inhibition on apoptotic sensitization to cytokines in LNCaP and PCc-3 prostate cancer cells. *J Interferon Cytokine Res* 21: 313-322, 2001.
20. Samaan N, Zhong Q, Fernandez J, Chen G, Hussain AM, Zheng S, Wang G and Chen QH: Design, synthesis, and evaluation of novel heteroaromatic analogs of curcumin as anti-cancer agents. *Eur J Med Chem* 75: 123-131, 2014.
21. Mazumder A, Gould M, Taurin S, Nicholson H and Rosengren R: Raloxifene potentiates the cytotoxicity induced by RL91, a second generation curcumin analog, in PC3 prostate cancer cells. *Toxicologist* 132: 146, 2013.
22. Zhang X, Chen M, Zou P, Kanchana K, Weng Q, Chen W, Zhong P, Ji J, Zhou H, He L, *et al*: Curcumin analog WZ35 induced cell death via ROS-dependent ER stress and G2/M cell cycle arrest in human prostate cancer cells. *BMC Cancer* 15: 866, 2015.
23. Lin L, Hutzen B, Ball S, Foust E, Sobo M, Deangelis S, Pandit B, Friedman L, Li C, Li PK, *et al*: New curcumin analogues exhibit enhanced growth-suppressive activity and inhibit AKT and signal transducer and activator of transcription 3 phosphorylation in breast and prostate cancer cells. *Cancer Sci* 100: 1719-1727, 2009.
24. Chiu TL and Su CC: Curcumin inhibits proliferation and migration by increasing the Bax to Bcl-2 ratio and decreasing NF-kappaBp65 expression in breast cancer MDA-MB-231 cells. *Int J Mol Med* 23: 469-475, 2009.
25. Wong RS: Apoptosis in cancer: From pathogenesis to treatment. *J Exp Clin Cancer Res* 30: 87, 2011.
26. Khan N, Adhami VM and Mukhtar H: Apoptosis by dietary agents for prevention and treatment of prostate cancer. *Endocr Relat Cancer* 17: R39-R52, 2010.
27. Mandalapu D, Saini KS, Gupta S, Sharma V, Yaseen Malik M, Chaturvedi S, Bala V, Hamidullah, Thakur S, Maikhuri JP, *et al*: Synthesis and biological evaluation of some novel triazole hybrids of curcumin mimics and their selective anticancer activity against breast and prostate cancer cell lines. *Bioorg Med Chem Lett* 26: 4223-4232, 2016.
28. Wei X, Du ZY, Cui XX, Verano M, Mo RQ, Tang ZK, Conney AH, Zheng X and Zhang K: Effects of cyclohexanone analogues of curcumin on growth, apoptosis and NF- κ B activity in PC-3 human prostate cancer cells. *Oncol Lett* 4: 279-284, 2012.
29. Oliver KM, Taylor CT and Cummins EP: Hypoxia. Regulation of NFkappaB signalling during inflammation: The role of hydroxylases. *Arthritis Res Ther* 11: 215, 2009.
30. Walmsley SR, Print C, Farahi N, Peyssonnaud C, Johnson RS, Cramer T, Sobolewski A, Condliffe AM, Cowburn AS, Johnson N, *et al*: Hypoxia-induced neutrophil survival is mediated by HIF-1 α -dependent NF-kappaB activity. *J Exp Med* 201: 105-115, 2005.
31. Maxwell PJ, Gallagher R, Seaton A, Wilson C, Scullin P, Pettigrew J, Stratford IJ, Williams KJ, Johnston PG and Waugh DJ: HIF-1 and NF-kappaB-mediated upregulation of CXCR1 and CXCR2 expression promotes cell survival in hypoxic prostate cancer cells. *Oncogene* 26: 7333-7345, 2007.
32. Suh J, Payvandi F, Edelstein LC, Amenta PS, Zong WX, Gélinas C and Rabson AB: Mechanisms of constitutive NF-kappaB activation in human prostate cancer cells. *Prostate* 52: 183-200, 2002.
33. Abdulghani J, Gu L, Dagvadorj A, Lutz J, Leiby B, Bonuccelli G, Lisanti MP, Zellweger T, Alanen K, Mirtti T, *et al*: Stat3 promotes metastatic progression of prostate cancer. *Am J Pathol* 172: 1717-1728, 2008.
34. Lindholm PF, Bub J, Kaul S, Shidham VB and Kajdacsy-Balla A: The role of constitutive NF-kappaB activity in PC-3 human prostate cancer cell invasive behavior. *Clin Exp Metastasis* 18: 471-479, 2000.
35. Lessard L, Bégin LR, Gleave ME, Mes-Masson AM and Saad F: Nuclear localisation of nuclear factor-kappaB transcription factors in prostate cancer: An immunohistochemical study. *Br J Cancer* 93: 1019-1023, 2005.
36. Domingo-Domenech J, Oliva C, Rovira A, Codony-Servat J, Bosch M, Filella X, Montagut C, Tapia M, Campás C, Dang L, *et al*: Interleukin 6, a nuclear factor-kappaB target, predicts resistance to docetaxel in hormone-independent prostate cancer and nuclear factor-kappaB inhibition by PS-1145 enhances docetaxel antitumor activity. *Clin Cancer Res* 12: 5578-5586, 2006.
37. Ross JS, Kallakury BV, Sheehan CE, Fisher HA, Kaufman RP Jr, Kaur P, Gray K and Stringer B: Expression of nuclear factor- κ B and I κ B α proteins in prostatic adenocarcinomas: Correlation of nuclear factor- κ B immunoreactivity with disease recurrence. *Clin Cancer Res* 10: 2466-2472, 2004.
38. Chakraborty M, Qiu SG, Vasudevan KM and Rangnekar VM: Par-4 drives trafficking and activation of Fas and FasL to induce prostate cancer cell apoptosis and tumor regression. *Cancer Res* 61: 7255-7263, 2001.
39. Jin R, Sterling JA, Edwards JR, DeGraff DJ, Lee C, Park SI and Matusik RJ: Activation of NF-kappa B signaling promotes growth of prostate cancer cells in bone. *PLoS One* 8: e60983, 2013.
40. Huang S, Pettaway CA, Uehara H, Bucana CD and Fidler IJ: Blockade of NF-kappaB activity in human prostate cancer cells is associated with suppression of angiogenesis, invasion, and metastasis. *Oncogene* 20: 4188-4197, 2001.
41. Yang CH, Yue J, Sims M and Pfeffer LM: The curcumin analog EF24 targets NF- κ B and miRNA-21, and has potent anticancer activity in vitro and in vivo. *PLoS One* 8: e71130, 2013.
42. Olivera A, Moore TW, Hu F, Brown AP, Sun A, Liotta DC, Snyder JP, Yoon Y, Shim H, Marcus AI, *et al*: Inhibition of the NF- κ B signaling pathway by the curcumin analog, 3,5-Bis(2-pyridinylmethylidene)-4-piperidone (EF31): Anti-inflammatory and anti-cancer properties. *Int Immunopharmacol* 12: 368-377, 2012.
43. Jorissen RN, Walker F, Pouliot N, Garrett TP, Ward CW and Burgess AW: Epidermal growth factor receptor: Mechanisms of activation and signalling. *Exp Cell Res* 284: 31-53, 2003.
44. Nicholson RI, Gee JM and Harper ME: EGFR and cancer prognosis. *Eur J Cancer* 37 (Suppl 4): S9-S15, 2001.

45. Di Lorenzo G, Tortora G, D'Armiento FP, De Rosa G, Staibano S, Autorino R, D'Armiento M, De Laurentiis M, De Placido S, Catalano G, *et al*: Expression of epidermal growth factor receptor correlates with disease relapse and progression to androgen-independence in human prostate cancer. *Clin Cancer Res* 8: 3438-3444, 2002.
46. Kim JH, Xu C, Keum YS, Reddy B, Conney A and Kong AN: Inhibition of EGFR signaling in human prostate cancer PC-3 cells by combination treatment with β -phenylethyl isothiocyanate and curcumin. *Carcinogenesis* 27: 475-482, 2006.
47. Shinde SR and Maddika S: PTEN modulates EGFR late endocytic trafficking and degradation by dephosphorylating Rab7. *Nat Commun* 7: 10689, 2016.
48. Rush JS, Quinalty LM, Engelman L, Sherry DM and Ceresa BP: Endosomal accumulation of the activated epidermal growth factor receptor (EGFR) induces apoptosis. *J Biol Chem* 287: 712-722, 2012.
49. Dillon RL, White DE and Muller WJ: The phosphatidylinositol 3-kinase signaling network: Implications for human breast cancer. *Oncogene* 26: 1338-1345, 2007.
50. Vivanco I and Sawyers CL: The phosphatidylinositol 3-Kinase AKT pathway in human cancer. *Nat Rev Cancer* 2: 489-501, 2002.
51. Graff JR, Konicek BW, McNulty AM, Wang Z, Houck K, Allen S, Paul JD, Hbaliu A, Goode RG, Sandusky GE, *et al*: Increased AKT activity contributes to prostate cancer progression by dramatically accelerating prostate tumor growth and diminishing p27Kip1 expression. *J Biol Chem* 275: 24500-24505, 2000.
52. Shimizu Y, Segawa T, Inoue T, Shiraishi T, Yoshida T, Toda Y, Yamada T, Kinukawa N, Terada N, Kobayashi T, *et al*: Increased Akt and phosphorylated Akt expression are associated with malignant biological features of prostate cancer in Japanese men. *BJU Int* 100: 685-690, 2007.
53. Morgan TM, Koreckij TD and Corey E: Targeted therapy for advanced prostate cancer: Inhibition of the PI3K/Akt/mTOR pathway. *Curr Cancer Drug Targets* 9: 237-249, 2009.
54. Ayala G, Thompson T, Yang G, Frolov A, Li R, Scardino P, Ohori M, Wheeler T and Harper W: High levels of phosphorylated form of Akt-1 in prostate cancer and non-neoplastic prostate tissues are strong predictors of biochemical recurrence. *Clin Cancer Res* 10: 6572-6578, 2004.
55. Kreisberg JI, Malik SN, Prihoda TJ, Bedolla RG, Troyer DA, Kreisberg S and Ghosh PM: Phosphorylation of Akt (Ser473) is an excellent predictor of poor clinical outcome in prostate cancer. *Cancer Res* 64: 5232-5236, 2004.
56. Mimeault M, Johansson SL and Batra SK: Pathobiological implications of the expression of EGFR, pAkt, NF- κ B and MIC-1 in prostate cancer stem cells and their progenies. *PLoS One* 7: e31919, 2012.
57. Song MS, Salmena L and Pandolfi PP: The functions and regulation of the PTEN tumour suppressor. *Nat Rev Mol Cell Biol* 13: 283-296, 2012.
58. Pópulo H, Lopes JM and Soares P: The mTOR signalling pathway in human cancer. *Int J Mol Sci* 13: 1886-1918, 2012.
59. Kremer CL, Klein RR, Mendelson J, Browne W, Samadzadeh LK, Vanpatten K, Highstrom L, Pestano GA and Nagle RB: Expression of mTOR signaling pathway markers in prostate cancer progression. *Prostate* 66: 1203-1212, 2006.
60. Liu G, Zhang Y, Bode AM, Ma WY and Dong Z: Phosphorylation of 4E-BP1 is mediated by the p38/MSK1 pathway in response to UVB irradiation. *J Biol Chem* 277: 8810-8816, 2002.
61. Haystead TA, Haystead CM, Hu C, Lin TA and Lawrence JC Jr: Phosphorylation of PHAS-I by mitogen-activated protein (MAP) kinase. Identification of a site phosphorylated by MAP kinase in vitro and in response to insulin in rat adipocytes. *J Biol Chem* 269: 23185-23191, 1994.